

Determination of Breakup Initial Conditions

Darren S. McKnight*

Kaman Sciences Corporation, Alexandria, Virginia 22303

The collisional fragmentation of a satellite via hypervelocity impact has garnered increasing attention as the on-orbit cataloged population has grown and various large-scale space systems have begun to be developed. Mass, number, velocity, and ballistic coefficient distributions of the resulting debris from a collision encounter have been modeled with limited empirical data. A review of this data is provided to clearly explain its function and limitations. The lack of empirical data in addition to the inability of laboratory experiments to replicate the mass and velocity of many on-orbit collision events hamper improvements to the relationships currently used.

Nomenclature

A, B	= constants, velocity distribution
a, b	= constants, power law
BC	= ballistic coefficient, m^2/kg
$ba1$	= constant, power law when $a = 1$
C_d	= coefficient of drag
CN	= cumulative number of fragments with mass greater than m_f
c, d, e	= constants, parabola
D	= object diameter, m
d	= ejecta diameter, m
d_m	= $(E_p)^{1/3}/6.194 \times 10^7$, m
E_p	= projectile energy, J
f, g	= constants, ballistic coefficient distribution
k	= proportionality constant, s^2/km^2
M	= mass, g
M_b	= breakup mass ($M_t - M_e$)
M_e	= ejecta mass, g
M_f	= fragment mass, g
M_p	= projectile mass
M_t	= target mass, g
N_0	= number of explosive fragments
$no. > 0.001M_t$	= number of fragments with mass greater than $0.001M_t$
RCS	= radar cross section, m^2
T, U	= constants, exponential
u	= Mott fragmentation parameter, g
V	= collision velocity, km/s
V_p	= projectile velocity, km/s
X	= average cross-sectional area

Introduction

AS the cataloged population of Earth-orbiting objects grows, large-scale space systems are proposed, and increased launch rates are projected, the collision hazard in low Earth orbit (LEO) will probably increase. An encounter between an operational satellite and a piece of debris with anticipated closing velocities in the 2–15 km/s range may damage or destroy the satellite, creating many more fragments. The cloud of debris produced by such an event defines the initial conditions (IC) for hazard assessment programs.

High fidelity ICs are essential to accurate hazard assessments, long term and short term. The key parameters of the

breakup IC are velocity, mass, number, and ballistic coefficient distributions. The velocity distribution of the cloud determines its time/spatial evolution whereas the mass relationship prescribes the lethality of a future impact. The ballistic coefficient distribution has a secondary effect on both the cloud's evolution under the influence of atmospheric drag and the lethality of the fragments. The historical development and limitations of existing relationships used for these purposes will be described. Collision-induced fragmentations and explosion events are both addressed. Throughout this article momentum transfer for collisions is assumed to be negligible. This assumption has been validated by the limited on-orbit and laboratory evidence.^{8,35,36} However, the examination of momentum transfer effects on the form and application of the relationships developed in this paper is necessary.

Mass Distributions

In 1975, T. Dale Bess (NASA Langley Research Center) reported on mass distributions from hypervelocity impacts.^{1,2} The studies analyzed two impact tests of aluminum and steel projectiles into a simulated spacecraft wall. The wall was an "insulated fiberglass wall in back of which were a number of electronics boxes containing resistors, capacitors, etc."¹ The projectile for the first test was a steel 1.65 g, 0.56 cm diam cylinder that had a measured velocity of 3.0 km/s. The projectile for the second test was an aluminum 0.37 g, 0.56 cm diam cylinder with an estimated impact velocity of 4.5 km/s. The resulting fragment masses ranged from 1 down to 10^{-7} g. The debris from each test was separated into five samples by mass. The data from this compilation are shown in Table 1.

The data for Table 1 were determined by collecting similarly sized fragments into the five groups and determining the total mass of each sample. This sample mass was then divided by an average fragment mass to yield the total number of fragments for each of the five data points (samples).

The fragment data for the two tests were fit to a power law curve:

$$CN = a(M_f)^{-b} \quad (1)$$

The b term drives the slope of the mass distribution curve while the a parameter simply shifts the curve along the y axis (cumulative number axis). The b terms for the two tests were 0.80 and 0.84, respectively, with a residual standard error of approximately ± 0.1 .² The a terms were 7.32 and 4.06, respectively. The total amount of debris produced (ejecta mass) from these two tests were 13.85 and 8.20 g, respectively.

NASA scientists modified the power law as derived in Ref. 1 by normalizing the mass term with the ejecta mass³:

$$CN = a(M_f/M_e)^{-b} \quad (2)$$

Received Dec. 7, 1990; presented as Paper 91-0299 at the AIAA 29th Aerospace Sciences Meeting, Reno, NV, Jan. 7–10, 1991; revision received Feb. 22, 1991; accepted for publication Feb. 25, 1991. This paper is declared a work of the U.S. Government and is not subject to copyright protection in the United States.

*Associate Senior Scientist, 2560 Huntington Ave., #200. Member AIAA.

Table 1 Mass distribution data¹

Limiting fragment mass, g	Test no. 1, number of fragments	Test no. 2, number of fragments
1.7×10^{-7}	1.9×10^6	1.7×10^6
2.4×10^{-5}	33,000	25,000
9.5×10^{-4}	2,000	1,600
4.4×10^{-2}	66	75
5.8×10^{-1}	—	5
8.8×10^{-1}	9	—

Application of Eq. (2) to the data from Bess changed the a terms to 0.89 and 0.69, respectively, while not changing the b parameter or slope.

The debris produced from the cratering or penetration of a large target via hypervelocity impact has been shown to follow a power law that is dependent on the amount of ejected mass. In 1978, assuming an impact velocity of 10 km/s, physical limits were presented for mass ratios (M_p/M_t) leading to catastrophic collisions and the debris produced (M_e).³ Tests on basalt, glass, and 1100-0 aluminum targets yielded power law mass distributions for the ejected debris similar to those developed by Bess.³ By scaling data from an impact of a 6 g plastic projectile at about 7–8 km/s into a large aluminum block, it was determined that an impactor (at 10 km/s) need only be 1/115 the mass of the satellite (assuming that the satellite has properties similar to an aluminum block) to cause a catastrophic fragmentation.⁴ Likewise, it was reported that the ejecta mass for an on-orbit collision between a small fragment and the assumed satellite would amount to 115 times the impactor's mass (at 10 km/s).³ Finally, the mass distribution was defined as

$$CN = 0.8(M_f/M_e)^{-0.8} \quad (3)$$

NASA scientists continued to refine the collisional breakup models by redefining ejecta mass and analyzing some new empirical impact data.⁵ The mass of the ejecta is now defined as

$$M_e = kV^2 = M_p \quad (4)$$

Equation (4) is a direct result of the fact that the mass of ejecta from an impact is proportional to the projectile's kinetic energy, and for a 10 km/s impact the V^2 term is close to the 115 factor posed in Ref. 3. A new power law relationship was developed using test data from two new experiments.⁶ The functional form appeared in Ref. 5

$$CN = 0.4478(M_f/M_e)^{-0.7496} \quad (5)$$

The data used to derive Eq. (5) came from shots 5192 and 5268 of a series of tests conducted at Arnold Engineering Development Center (AEDC), Range G. The target for each test was a hollow aluminum cylinder ($L = 99$ cm, $D = 28$ cm) with electronic boxes attached inside at various locations. The total mass of 26 kg was 31% aluminum and 69% circuit boards. The projectile was a 237 g aluminum/Lexan tubular plug ($L = 5.8$ cm, $D = 5.3$ cm). The impactor struck the broadside of the target at its center of mass at 5.9 and 3.3 km/s, respectively. These tests were 2 of 19 experiments conducted "to assess the damage that would occur upon the impact of a high speed projectile with a composite target."⁶

Figure 1 shows the data for shot 5192 plotted against two different power law combinations. Because of documented contamination of the debris in the test chamber and uncertainty in the impact velocity for shot 5268,⁶ its data are not reproduced.

One difficulty in the evaluation of the constants in the power law relationship is the limited amount of empirical data

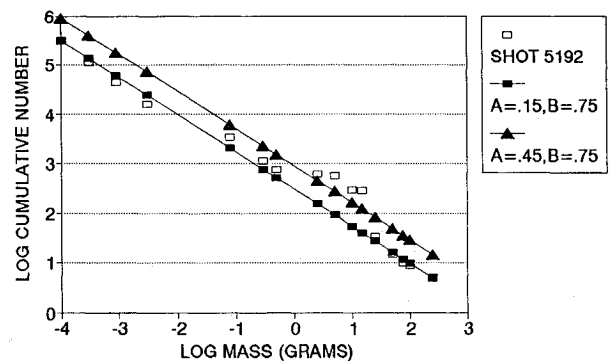


Fig. 1 Data from shot 5192 are approximated well by a power law relationship. Two possible power law curves are shown.

available. The Air Force Academy teamed with the Air Force Armament Laboratory, Space Weapons Lethality (SAA) Branch to help correct this deficiency. Three major efforts were initiated in 1988: 1) analyze data from ongoing lethality tests, 2) search for unanalyzed, existing data from previous impact tests, and 3) develop a dedicated test solely for debris characterization.

First, the analysis of lethality tests from 1988–90 provided valuable insights into the breakup of spacecraft-type structures by hypervelocity impact.⁸ Fragmentation debris was collected, counted, and fit to a variety of mathematical relationships that included the power law, parabola, hyperbola, and arctangent. During this effort the parabola was found to yield the best curve fit results for the available empirical data. The recent data exhibited a rounding off in the smaller masses. This may be due to fewer fragments being produced or fewer being collected. More experiments are needed to clearly determine the cause of this leveling off of the mass distribution curve. The parabola takes the form

$$\log(CN) = c - d [\log(M_f/M_t) + e]^2 \quad (6)$$

It should be noted that M_t has replaced M_e in the mass ratio term of Eq. (6). This implies that the mass distribution for the entire structure may be represented by a single curve.

The term c represents the log of the total number of pieces detected whereas e is set to $\log(M_m/M_t)$, where M_m is the smallest fragment mass reliably found. These two parameters, thus, force the curve to be limited by the data used to derive it, emphasizing interpolation between data points over extrapolation outside of the test data range. To use the parabola to extrapolate, a conscious decision must be made to change the parameters or go past the apex of the parabola. On the other hand, the power law may be easily used to extrapolate to mass ranges well below those collected during data reduction. Until the breakup phenomenology of a spacecraft structure is better understood, users must be cautioned not to extrapolate mass distribution relationships beyond the limits of the collected data or to scale data without a thorough understanding of the process. The wide variety of values found for the b term in the power law in Ref. 8 makes this note even more important since a very small change in b will cause vastly different values for the number of small debris produced.

The estimation of error for data will affect the values of a and b of the power law.⁷ Assuming a constant error for all mass sizes will generally produce a shallower slope (smaller b). Assignment of a larger error to the smaller mass data generally results in a steeper slope (larger b). The value of b may change by as much as 50% (e.g., from 0.4 to 0.6) by merely using a different error estimation scheme. Additionally, the uncertainty in the data does not warrant the use of four significant figures in the values of a and b .

The constants for both the power law (a, b) and the parabola (c, d, e) are determined for 10 catastrophic impact

events in Table 2, which lists this data and a short descriptor for each test. A new constant, $ba1$, is included under the power law column. The parameter $ba1$ is simply b when $a = 1$.

From Table 2, it can be seen that a varies from 0.1 to 17 whereas b ranges from 0.3 to 1.1, respectively. Generally, as a gets larger, b gets smaller and vice versa. The $ba1$ consistently remains in the 0.6–0.8 range even though it provides a slightly worse curve fit. Aerospace Corporation uses a range of b values in their analyses: $b = 0.4$ for rigid material and $b = 0.8$ for nonrigid material.⁹ In actuality, using a Chi square goodness of fit test yields 0% confidence for all power law representations even though the power law provided a very good representation of the data from Table 1. The parabola fits were much better with confidence levels from 20 to 90% with an average of about 70%. For the parabola, the constants c , d , and e had ranges of 2.1–4.4, 0.1–0.8, and 3.0–7.4, respectively.

The major difference between the parabola and the power law is in the estimation of the number of small fragments produced. The power law predicts an increasing number of small fragments whereas the parabola fewer. Figure 2 plots two power law curves and a parabola against impact data from CU5271, which will be discussed later.⁷ Note the large difference in the number of small fragments produced by changing from the steep to the shallow power law. At this time, it is uncertain whether the leveling off of the curve is a function of inability to collect smaller debris or a true representation of the breakup process. Yet, it is a certainty that at some point the mass distribution curve will level off (i.e., smaller and smaller pieces cannot continue to be produced in increasing amounts indefinitely).

The parabola provides the flexibility to account for data showing a leveling effect in the smaller masses if, when debris collection techniques are improved, it is found to follow such a distribution. Another option in this regard, depending on how the empirical data looks, would be to clearly define a lower mass limit for using the power law. It is unclear how these mass distributions scale, and attempts to do so must be supported by more laboratory work.

A hyperbolic mass distribution relationship was also investigated: the hyperbola has 5 degrees of freedom (vs 2 for the power law and 3 for the parabola) and fit all empirical mass distribution data with 90–100% confidence.⁸ Yet, the hyperbola was very difficult to work with, and its coefficients had no physical meaning so it is not currently being considered.

A very important consideration for any mass distribution is that mass is conserved. That is to say, the sum of the fragments produced should equal the original mass of the target.

An in-house analysis was conducted by the Air Force Academy for the Air Force Armament Laboratory to assess the usefulness of soft catch media as instrumentation for impact tests.¹⁰ Ten 230 cm² square (0.5 in. thick) styrofoam tiles were mounted in the interior of the test chamber (Range G AEDC) during shot 6470 (described as CU6470 in Table 2). The sampling of fragment captures in the 10 μ and 1 mm size bins were compared to predicted numbers from the "standard" power law ($a = 0.45$, $b = 0.75$). The average number of 10 μ and 1 mm fragments calculated from the sampling was 1.6×10^5 and 2900, whereas the power law, parabola, and

hyperbola estimated $1.6 \times 10^{11}/23,000$, $3.0 \times 10^6/8700$, and $2.5 \times 10^4/1300$, respectively. The use of the parabola requires an iterative approach that insures that previous estimates of large fragments are not corrupted by estimating the number of smaller fragments. More research must be conducted to insure that a large portion of the small fragments produced did not remain uncounted because they were moving too slowly or too quickly to be captured within the softcatch tile. Future hypervelocity impact tests at Range G will also use more tiles to provide a greater sampling of the debris cloud spatially.

Present theory assumes that if the energy of the projectile is large enough to cause complete fragmentation of a target, the ejecta mass follows a power law and the remainder breaks up as an explosion. The hypothesized mass distribution for an explosion is an exponential relationship developed from an Atlas tank fragmentation.^{5,11} Analysis of a wide variety of explosions have provided insights into other aspects of explosion-induced breakups.¹² The curves derived from the single explosion event are represented in Eqs. (7a) and (7b):

$$CN = 1.71 \times 10^{-4} M_b \exp(-0.02056 M_f^{1/2}) > 1936 \text{ g} \quad (7a)$$

$$CN = 8.69 \times 10^{-4} M_b \exp(-0.05756 M_f^{1/2}) < 1936 \text{ g} \quad (7b)$$

The mass available for breakup M_b is the mass of the target minus the ejecta mass. The amount of ejecta was defined earlier as a function of the impact velocity and projectile mass, but it also may be prescribed as a percentage of the target mass to parameterize breakup results.^{9,15}

An analysis conducted by the Defence Research Establishment Valcartier examined the fragments produced in three sets of five identical explosion experiments.¹³ Identical amounts of high explosive were used to fragment precisely machined metallic casings of different materials. The form of the debris mass distribution as given by Mott is similar to Eqs. (7a) and (7b):

$$CN = N_0 \exp[-(M_f/u)^{1/2}] \quad (8)$$

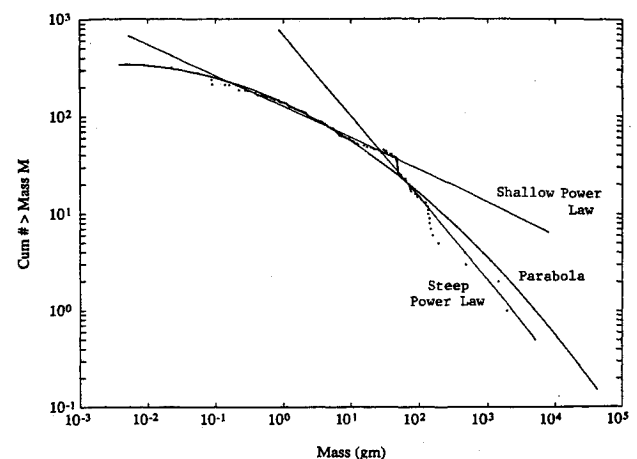


Fig. 2 Parabola levels off as smaller fragment masses are encountered while the power law continues to predict more smaller pieces. Plotted data are from CU-5271.⁷

Table 2 Lethality test results⁸

Name	M_t , kg	M_p , g	v_p , km/s	Power a, b ($ba1$)	Parabola c, d, e
GRC 381 (spherical Al tank)	0.027	1.6	6.4	10, 0.4 (0.7)	2.6, 0.2, 4.4
GRC 385 (spherical Al tank)	0.027	1.6	6.4	17, 0.3 (0.7)	2.6, 0.2, 4.4
PSI 5268 (cylindrical structure)	26	237	3.3	2.0, 0.6 (0.6)	2.7, 0.5, 4.4
PSI 5192 (cylindrical structure)	26	237	5.9	0.4, 0.7 (0.7)	4.4, 0.1, 7.4
GRC 6380 (spherical Al tank)	2.1	81	5.5	3.7, 0.4 (0.6)	2.5, 0.3, 4.0
GRC 6384 (spherical Al tank)	2.1	81	5.5	0.4, 0.7 (0.6)	2.1, 0.7, 3.0
GRC 6385 (spherical Al tank)	2.1	81	5.5	0.1, 1.1 (0.7)	2.4, 0.4, 3.6
GRC 6386 (spherical Al tank)	2.1	81	5.5	0.8, 0.7 (0.7)	2.2, 0.8, 3.0
CU 6470 (two spherical Al tanks)	1.6	85	5.5	1.3, 0.7 (0.7)	2.9, 0.4, 4.4
1979-17 (satellite)	850	16,000	6.7	0.4, 1.0 (0.8)	2.4, 0.2, 4.4

Equations (7a) and (7b) may be written in the form

$$CN = TM_b \exp(-UM_f^{1/2}) \quad (9)$$

Relating the two forms, it is seen that $TM_b = N_0$ and $U = (1/u)^{1/2}$. Thus, TM_b simply represents the total number of fragments detected that will be largely a function of satellite structure, explosive location, and, if applicable, orbit of exploding satellite. The constant U represents the slope of the mass distribution curve when $\log(CN)$ is plotted against the square root of the fragment mass.

By converting all the data from Ref. 13 into the terminology of Eq. (9), it is found that the standard deviation for the two constants T and U are about 31 and 75% of their nominal mean values, respectively. These calculations were made from highly repeatable experiments, whereas the explosion of rocket bodies or the secondary breakup from a catastrophic collision will have more uncertainty due to different materials, structure, and loading conditions. For these reasons, it is assumed that the constants in Eqs. (7a) and (7b) will have at least as large uncertainties if they are to be used in the general manner as currently being applied by orbital debris analysts.

As a result, it is proposed that Eqs. (7a) and (7b) may be combined into one equation with T ranging from 1×10^{-4} to 1×10^{-3} with a nominal value of 5×10^{-4} , whereas U will have a nominal value of 0.04 with extremes of 0.02 and 0.06.

Recent analyses by TRW to simulate the fragmentation of a launch vehicle/rocket body in various scenarios hold promise for future models.³⁸ Using a purely analytic code, the mass distribution from the explosion of a Starbird Stage IV followed an exponential curve with $T = 4.5 \times 10^{-3}$ and $U = 0.45$. The debris also fit a power law very well with $\alpha = 1$ and $b = -0.83$.

Compilation of the data from the tests listed in Table 2 resulted in a new relationship that predicts the number of large mass fragments produced by an impact event⁸:

$$\text{no.} > 0.001M_t = 5(E_p/M_t)^{1/2} \quad (10)$$

Figure 3 plots the applicable data from Table 3 against this relationship with three sigma error bars. The data point for 1979-17 (on-orbit breakup) is suspect. The largest fragment from this event has remained in a very stable orbit, similar to what would have been expected if the satellite had not been fragmented. Thus, the fragments produced may have been from only a fraction of the total mass.

Yet, it is known that the relative kinetic energy goes into a variety of phenomena: heat, light, plastic work, fragmentation, and debris spread velocity. Aerospace Corporation scientists have developed an algorithm for how much of the relative kinetic energy is partitioned into the spread of debris fragments as a function of the mass ratio (m_p/m_t). If the two colliding objects are comparable in mass, the energy available for the spread of the debris is half of the available energy. If the projectile is small in comparison to the target, then all of the energy goes into the spread of debris and vice versa.¹⁵

The second source of data, analysis of debris from earlier tests, has proven very useful. The Air Force Armament Laboratory contracted the University of Colorado (Boulder) to

analyze several crates of debris from the series of tests from which Ref. 6 originated. There were a total of 19 test shots conducted that examined the effects of geometry of impact, pressurization, and projectile lethality. The debris from these tests has been housed at Physical Sciences Incorporated since the tests were conducted over 10 years ago. All the experiments had similar test conditions. Thus far, two shots have been analyzed by the University of Colorado (CU), 5271 and 5272.⁷ This data will be referred as CU5271 and CU5272. The results for power law and parabolic fits yielded similar results to previous experiments (i.e., the constants for the equations were generally within the ranges specified earlier). The mass distribution curve for CU5271 was best portrayed by a parabola, whereas for CU5272 the power law representation appeared most appropriate. Two data points representing these two tests are part of the plot shown in Fig. 3 as well as the tests listed in Table 2. Analysis by CU of more crates of test data is ongoing.

The last source of data, tests dedicated to debris collection, has not yet materialized. The general concept of constructing a test program of component and scale model testing around a spaceflight-ready test article has received community-wide support but little funding. Instrumentation that is capable of determining mass/velocity distributions numerically and spatially down to a fragment size of 1 mm would provide a much greater insight into breakup and debris generation processes. The proposed test was assigned the name Satellite Lethality and ASAT Modeling Test—the SLAM Test. Spacecraft 30290, part of the Oscar series Navy Navigation Satellite System, was provided to the Air Force Academy by the Chief of Naval Operations for laboratory testing in pursuit of improved breakup models.^{16,17}

In summary, there is much uncertainty in the mass distribution models currently used due to the limited amount of empirical data of questionable quality. The uncertainty in the laboratory data mainly results from possible incomplete collection of fragments and collateral fragmentation with the test chamber wall. Tests dedicated to determining more accurate representations of the debris resulting from a collision-induced fragmentation are required. For the time being the following observations are pertinent to any mass distribution debris modeling.

1) The power law is a simple, easy to use relationship that may be easily misused by extrapolation beyond the limited supporting data base.

2) The combined use of the power law and exponential equations to describe a breakup is also limited by the small experimental data base and does not provide a single curve representation for a single target.

3) The parabola may be an alternative that addresses concerns of previous models and more satisfactorily represents the breakup process, but it still requires validation, like the others, by much more empirical data acquired solely for this purpose.

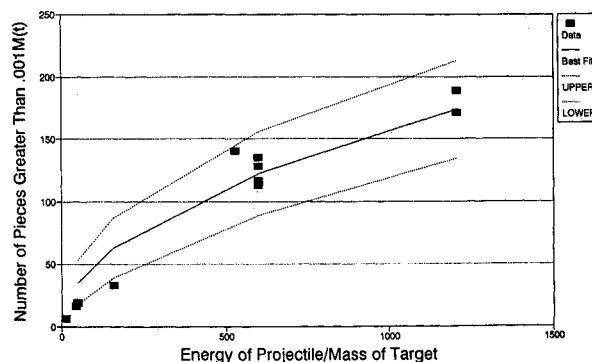


Fig. 3 This energy sensitive relationship relates a variety of test scenarios under one relationship in predicting the number of large fragments produced from an impact.⁸

Table 3 Diameter to mass conversion— f and g

Data source	f	g	Minimum D
Soviet on-orbit ³³	30,800	2.54	1.5 m
Assorted on-orbit ³	47,200	2.26	10 cm
Debris on-orbit ²⁸	22,900–23,500	3.63–3.81	10 cm
Debris on-orbit ²⁹	17,000–189,000	2.26	10 cm
CU6470 (lab) ⁷	8,100	2.13	1 mm
CU5271 (lab) ⁷	9,200	2.25	1 mm
CU5272 (lab) ⁷	64,600	2.63	1 mm
5192 and 5268 (lab) ⁶	47,000–140,000	2.26–3.00	1 mm

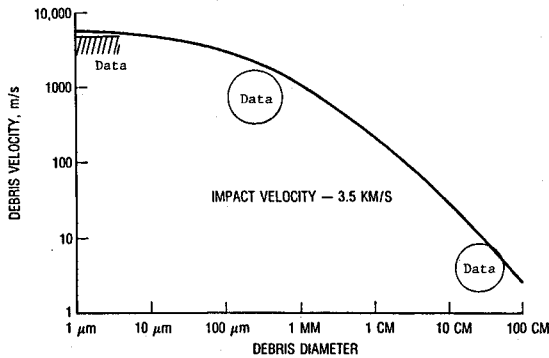


Fig. 4 Velocity distribution of debris from a hypervelocity collision ($V = 3.5$ km/s) was derived from little data, shown by the three small data regions.¹⁸

4) All the velocities encountered in the existing hypervelocity impact data base (3–7 km/s) are below the average (10 km/s) and maximum (15 km/s) impact velocities expected in LEO. The ability to scale the data to typical on-orbit debris encounters is suspect. There is much analytic work required to determine how and with what parameters scenarios may be accurately scaled: skin thickness, projectile mass, energy, momentum, etc. After appropriate research is conducted to determine these relationships, empirical data will have to be obtained to validate them.

Velocity Distribution

The acquisition of velocity distribution information is very difficult due to the high speeds and small size of ejecta coupled with the many contamination sources possible during a laboratory test. Bess^{1,2} originally reported in 1975 that the velocity of larger fragments from a hypervelocity impact were about 10 m/s whereas the very small fragments (10^{-7} g) from a collision could reach velocities on the order of 4–11 km/s.

The two tests analyzed in Ref. 6 provided some “fuzzy” data points for a velocity distribution curve. The data points were fit with a hypothetical curve describing the limiting (maximum) delta velocity as a function of fragment size.¹⁸ Figure 4 plots the best fit curve and data points from Ref. 6. This curve is described by the following equation¹⁹:

$$\log d = -6 - B/2A + [1/2A][B^2 + 4A(\log V - 3.76)]^{1/2} \quad (11)$$

where $A = -0.1022$ and $B = 0.0533$.

This equation was then scaled to account for varying impact velocities and to incorporate the observation that the maximum ejecta velocity is normally 1.3 times the relative projectile velocity for smaller debris.^{18,19} The resulting equation normalizes the velocity distribution to both the projectile velocity and energy^{20,21}:

$$\log(V/V_p) = A - B [\log(d/d_m)]^2, \quad \text{if } d > d_m \quad (12a)$$

and

$$\log(V/V_p) = A, \quad \text{if } d < d_m \quad (12b)$$

where $A = 0.225$ and $B = 0.1022$.

The value of A would be 0.1139 for $V = 1.3V_p$ while $A = 0.2225$ yields a ratio of 1.6. Thus, even though the accepted maximum velocity is $1.3V_p$, the equation above allows velocities as high as $1.6V_p$. For this reason, a range of A values will be suggested, 0.1–0.25. The lack of empirical data makes it difficult at this time to define a range for B , and it should be noted that the four significant figures of the B term do not imply high accuracy.

Whereas velocity information is often very difficult to obtain from laboratory tests, velocity data for large objects from

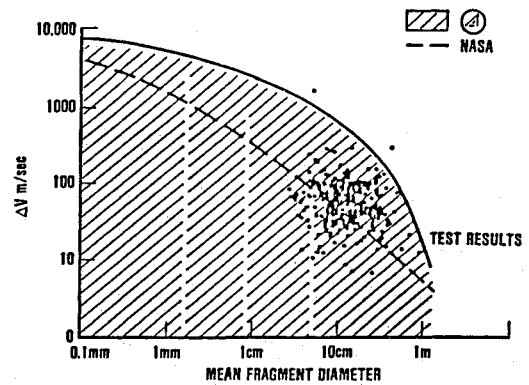


Fig. 5 Velocity data from the on-orbit collisional breakup of Satellite 1979-17 (or P78-1) compare favorably to the hand-drawn velocity distribution (solid line) and are centered about the nominal relationship (dotted line).¹⁴

on-orbit breakup events are fairly robust. Data analyzed from a variety of on-orbit breakups showed very good correlation with the model described above [Eqs. (12a) and (12b)].³² Data acquired from the collision breakup of 1979-17 are plotted on a velocity distribution curve scaled to the event by Aerospace Corporation scientists (Fig. 5).¹⁵ The dotted line is the velocity distribution as described by Eqs. (12a) and (12b) whereas the upper line was hand-drawn by scientists. All on-orbit breakup debris supports the use of the x axis as the lower boundary while Fig. 4 shows that the maximum velocity for a given size may exceed the model's prediction by as much as an order of magnitude.

On the other hand, modelers bound the velocity distribution by 1.3 and 0.1 of the nominal with a “triangular spreading function” between these extremes.²⁰ These limits were found to agree favorably with a number of on-orbit breakup events of both collisions and explosions.³² (Only two of these were considered collision induced.) Note that the velocity distribution curves are routinely provided as a function of size instead of mass. The conversion from size to mass will vary depending on satellite structure, type of data (lab vs on-orbit), and impact parameters. Techniques for this process will be covered in the next section on ballistic coefficients.

Debris analysts adjusted this “nominal” curve for a specific on-orbit collision event: D180 Test.¹⁴ Assuming that the larger fragments have equal kinetic energies imparted to them causes the round off of the curve for larger masses. For smaller fragments, however, the shock wave does not transmit its energy as effectively, so a leveling of the curve is predicted since smaller fragments have less kinetic energy transferred to them. Figure 6 plots these curves as a function of percentage of impactor relative kinetic energy that goes into fragment spread velocities. A higher percentage absorbed results in higher velocity components. The HOE (Homing Overlay Experiment) curve came from data on a suborbital hypervelocity impact test.^{14,23,24}

In summary, the major observation made for mass distributions also holds true for velocity distributions: more velocity data taken from more realistic tests are needed to refine present distributions.

Ballistic Coefficient Distribution

The ballistic coefficient (BC) is defined as

$$BC = C_d X/M \quad (13)$$

The BC of an object determines its response to atmospheric drag and is a measure of its compactness. A small BC object is more compact, thus is less affected by atmospheric drag and probably more lethal. The C_d term for an orbiting fragment is assumed to be about 2.2.²⁵ The calculation of BC for debris

fragments usually requires knowing both their area and mass. Yet, on-orbit debris may have their *BC* determined by their orbital decay pattern alone.^{27,28,41,42}

Calculation of effective average cross-sectional area (*X*) from radar cross section (*RCS*) coupled with an ability to determine an object's mass from *A* will essentially define an object well enough to ascertain how it will be affected by the atmosphere and how lethal it might be upon impact.

The first attempt at relating an *RCS* value to mass followed the Eq. (3):

$$M = 62,000 (RCS)^{1.13} \quad (14)$$

Equation (14) was derived from curve fitting data from over 30 on-orbit payloads and rocket bodies and debris fragments from an explosion of a Centaur rocket on Earth. The exponent for Eq. (14) was expected to lie between 1.0 (hollow structure) and 1.5 (solid structure).³ An analysis of on-orbit Soviet payloads and rocket bodies produced similar results.³³ Figure 7 plots data showing the range for each type of Soviet payload or rocket body. A best fit to the mean values yields constants of 40,500 and 1.27, respectively, with a correlation coefficient *r* of 0.97. Similar analysis of the breakup of the P78-1 solwind satellite yielded supporting results highlighting the difficulty of studying on-orbit debris data for this application.⁴¹

Assuming an average circular cross section with a diameter *D* (m), Eq. (14) becomes

$$M = 47,200(D)^{2.26} \quad (15)$$

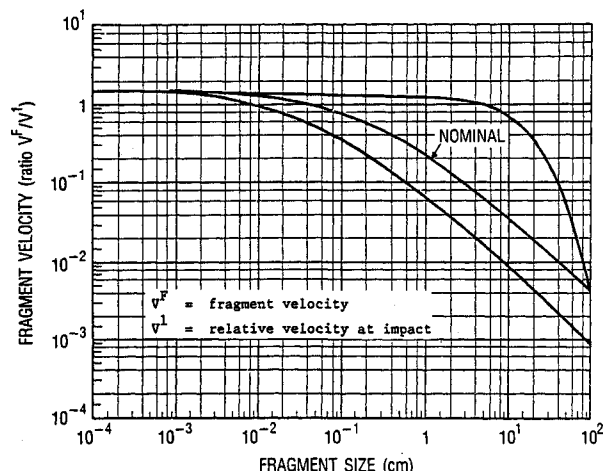


Fig. 6 Standard velocity distribution was modified to predict the debris cloud characteristics from the D180 Test. The curves are drawn as a function of the percentage of impactor energy that goes into the spread of the fragments. The lower curve is 10%, the nominal curve assumes 100% transfer, and the upper curve is a hand-drawn absolute limit.¹⁴

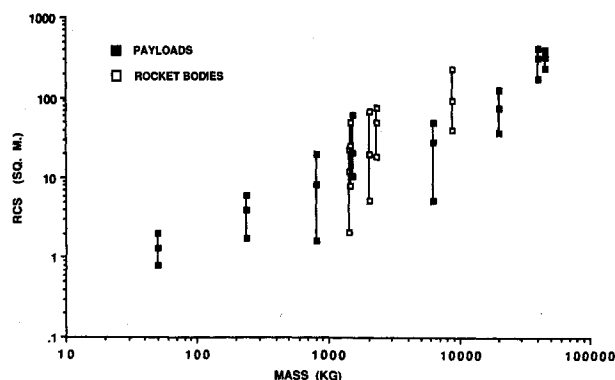


Fig. 7 Compilation of over 250 data points on 14 types of Soviet payloads and rocket bodies follow the relationship $m = 40,500(RCS)^{1.27}$ (Ref. 33).

The transition from *RCS* to *X* (and thus *D*) is fraught with uncertainties^{34,41,42} and, as a result, relationships developed to relate these parameters have representative large error bars²⁶:

$$X = 0.5712(RCS)^{0.7666 \pm 0.048} \quad (16a)$$

$$M = 37.97(X)^{1.86 \pm 0.044} \quad (16b)$$

$$M = (23.300 \pm 300)(D)^{3.72 \pm 0.088} \quad (16c)$$

Analysis of thousands of on-orbit fragments was used to build Eqs. (16a-16c). Similar reviews of debris from laboratory tests yield a wide range of values for the constants in Eqs. (15) and (16c) that are of the form

$$M = f(D)^g \quad (17)$$

Bounding the problem with *f* and *g* terms of 10,000-60,000 and 2.25-3.00, respectively, produces a wide range of possible *BC* values. For instance, a 1-cm-diam fragment may have a *BC* in the range 9.1×10^{-2} to $17 \text{ m}^2/\text{kg}$ using these limits, with a nominal value ($f = 45,000$, $g = 2.26$) of $0.13 \text{ m}^2/\text{kg}$. Actual *BC* values calculated for trackable debris from a variety of breakups ranged from 0.01 to $10 \text{ m}^2/\text{kg}$ with an average around $0.05\text{--}0.2 \text{ m}^2/\text{kg}$.^{28,29} The relationships above have combined debris from a variety of breakup events. Thus far, there has been no empirical data to support separate developments for different types of breakups.

An alternate analysis of on-orbit debris reveals a correlation between *f* and satellite structure.³⁰ The *f* term was found to be proportional to the "spacecraft density": satellite's dry mass divided by its approximate volume. Typical values of *f* ranged from 17,000 to 66,000 for U.S. rocket bodies and 55,000-189,000 for Soviet spacecraft. It was found that this factor will also vary as debris size changes. One approach is to halve the *f* term for every tenfold increase in fragment size, a smaller *f* for larger fragments.²⁹ Other studies have also identified larger *f* terms for smaller debris sizes as well as a larger *g* value.²⁰

In summary, assuming a circular cross section of debris on average the *BC* of a debris fragment may be found as a function of fragment diameter by

$$BC = (1728/f)D^{(2-g)} \quad (18)$$

where $f = 10,000\text{--}60,000$ (45,000 nominal) and $g = 2.25\text{--}2.50$ (2.26 nominal).

Equation (18) has not been validated. This relationship and similar previous equations must be used carefully to insure that mass is conserved when assigning characteristics to debris from a breakup. The ability to do this has not been a trivial task in earlier analyses.

The analysis of ballistic coefficient values has spanned significant on-orbit data, but still the correlation between *RCS* and *X* is poor in most cases. Additionally, a robust algorithm to adjust *f* and *g* for specific debris clouds is warranted. The combination of laboratory and on-orbit data provides a wide spectrum of results that show that the *BC* of debris fragments vary significantly about some nominal value.

Summary

The Appendix summarizes the most exercised and validated relationships used to define debris resulting from satellite breakups with appropriate cautions and disclaimers. There is a wide range of possible values for each aspect of the debris cloud, and only more testing coupled with development of new analytical/computational tools will be able to reduce the uncertainties. It is extremely important to note that the limited data base does not adequately address collisions with impact velocities in the 8-15 km/s range with moderate masses (100 g-1 kg) that are likely to occur between LEO objects. Therefore, more empirical and analytical work is required to

better understand how to scale available data to these scenarios, though a recent report has shown good promise in scaling phenomenology.³⁷ On the other hand, planned on-orbit or suborbital weapons tests are slated to occur in the 1–4 km/s range in an attempt to minimize debris. The distributions in the Appendix should be used when hazard assessments are conducted for operational spacecraft.³¹

Appendix: Mass/Velocity/BC Distributions

Mass

Power Law

$CN = a(M_f/M_e)^{-b}$ for ejecta $a = 0.3$ – 1.1 (nominal 1.0) and $b = 0.4$ – 0.7 (nominal 0.65).

1) If $10 V^2 M_p > M_t$ (V in km/s), then impact is considered catastrophic and $M_e = M_t$; basis for catastrophic limit is qualitative only.

2) It is assumed that $m_e = 10 V^2 M_p$ follows the power law and the remainder of the structure, $M_b = M_t - M_e$, breaks up in an exponential distribution if the encounter is considered catastrophic.

3) Easy to use but be careful extrapolating to small masses; relationship may overestimate number of small fragments.

4) When using any mass distribution, insure that mass is conserved.

Exponential

$$(\text{Explosion}) CN = TM_b \exp(-UM_f^{1/2})$$

where $T = 1 \times 10^{-4}$ – 1×10^{-3} (nominal 5×10^{-4}) and $U = 0.02$ – 0.06 (nominal 0.04).

1) Equation is the result of addressing uncertainties plus having only one real data set.

2) When using any mass distribution, insure that mass is conserved.

Parabola

$$\log(CN) = c - d[\log(M_f/M_t) + e]^2$$

where $c = 2.1$ – 4.4 (nominal 2.5), $d = 0.1$ – 0.8 (nominal 0.4), and $e = 3.0$ – 7.4 (nominal 4.4).

1) Roundoff at low mass limits small debris to empirical results and prevents extrapolating beyond valid range without a conscious decision to do so. Extrapolating to small masses requires a cumbersome and iterative process.

2) Be careful extrapolating to small masses; relationship may underestimate number of small fragments.

3) Single curve for entire distribution avoids need to combine power and exponential laws.

4) When using any mass distribution, insure that mass is conserved.

Large Pieces

$$\text{no.} > 0.001 M_t = 5 (E_p/M_t)^{1/2}$$

1) Energy sensitive relationship provides unique analytical tool, but effect of target structure, impact point, and projectile characteristics are unknown.

2) Units of E_p/M_t are J/g.

Velocity

$$\log(V/V_p) = A - B[\log(d/d_m)]^2, \text{ if } d > d_m$$

$$\log(V/V_p) = A, \text{ if } d < d_m$$

where v = limiting debris velocity, m/s, $A = 0.1$ – 0.25 , $B = 0.1022$, $d_m = (E_p)^{1/2}/6.194 \times 10^7$, E_p = kinetic energy of projectile, J, and V_p = velocity of projectile, m/s.

1) The value of A determines the maximum value for the velocity distribution while it is bounded on the low number end by the x axis.

2) Distribution is bounded by 1.3 and 0.1 of nominal curve with a triangular spreading function between these extremes by NASA.²⁰

3) Relationships for upper and lower bounds may be hand-drawn about nominal curve for a specific event as was accomplished for the D180 Test.¹⁴

Ballistic Coefficient

$$BC = (1728/f)D^{(2-g)}$$

$$[M = f(D)^g \text{ and } X = 0.5712 (RCS)^{0.7661 \pm 0.048}]$$

$$f = 10,000\text{--}60,000 \text{ (nominal 45,000)}$$

$$g = 2.25\text{--}3.00 \text{ (nominal 2.26)}$$

1) Conversion from RCS to physical cross section is suspect as well as the RCS to mass conversion.

2) BC conversions vary by satellite structure and fragment size, but there is no robust technique outlined to cover full range.

Acknowledgments

The Air Force Armament Laboratory, Space Weapon Lethality Branch (AFATL/SAA), has sponsored research into orbital debris analysis at the Air Force Academy for the last three years. Their financial and technical support has resulted in many scientific improvements in this field, especially in the advancement of an understanding of the satellite breakup process. Christopher B. Brechin, Scientific Atlanta, provided valuable insights in the early stages of this effort. A special thanks is extended to the Air Force Academy for their continued support of our endeavors to address the issues covered in this report and to Pat Ridley for her continued prompt and professional support. The comments by Nicholas Johnson (Teledyne Brown Engineering), Vladimir Chobotov (The Aerospace Corporation), and Donald Kessler (NASA Johnson Space Center) during the refining of this paper have insured that it represents a valuable consensus of the debris community. The publication of this paper was partially funded under the Defense Nuclear Agency Orbital Debris Breakup Modeling Program.

References

- Bess, T. D., "Mass Distribution of Orbiting Man-Made Space Debris," NASA TN D-8108, Dec. 1975.
- Bess, T. D., "Size Distribution of Fragment Debris Produced by Simulated Meteoroid Impact on Spacecraft Wall," NASA SP-379, 1975.
- Kessler, D. J., and Cour-Palais, B. G., "Collision Frequency of Artificial Satellites: The Creation of a Debris Belt," *Journal of Geophysical Research*, Vol. 83, No. A6, June 1978, pp. 2637–2646.
- Kessler, D., private communications, 1990.
- Su, S.-Y., and Kessler, D. J., "Contribution of Explosion and Future Collision Fragments to the Orbital Debris Environment," *Advances in Space Research*, Vol. 5, No. 2, 1985, pp. 25–34.
- Nebolsine, P. R., Lord, G. W., and Legner, H. H., "Debris Characterization Final Report," Physical Sciences Inc., Andover, MA, PSI-TR-399, Dec. 1983.
- MacLay, T., and Hinga, M., "Analysis of Shot CU-5272 Fragments," University of Colorado, Boulder, CO, Technical Memo prepared for Air Force Armament Laboratory Contract F-08635-89-k-0227, June 1990.
- McKnight, D. S., and Brechin, C., "Debris Creation via Hypervelocity Impact," AIAA Paper 90-0084, Jan. 1990.
- Chobotov, V. A., and Spencer, D. B., "Debris Evolution and Lifetime Following an Orbital Breakup," AIAA Paper 90-0085, Jan. 1990; see also *Journal of Spacecraft and Rockets*, to be published.
- McKnight, D. S., and Brechin, C. B., "Analysis of Shot 6470," U.S. Air Force Academy, Dept. of Physics, Colorado Springs, CO, Internal Memo, June 1989.
- Edwards, J. R., "Range Safety Considerations Related to Atlas Tank Fragmentation for the Penetration Aids Program for PMR," GDA-63-0048, May 1963.
- Loftus, J. P., Jr. (ed.), *Upper Stage Breakup Events*, AIAA, Washington, DC, 1989.
- Voyzelle, B., Belanger, S., and Bourget, C., "Evaluation of the Sampling and Recovery Techniques Developed for the Radar Frag-

mentation Characterization Method," Defence Research Establishment Valcartier, Canada, DREV R-44442/87, [(418)844-4271], Sept. 1987.

¹⁴Hagan, J., Follin, J., and Maras, J., "Delta 180 Program On-Orbit Safety Analysis Report," Johns Hopkins Univ., Applied Physics Lab., Laurel, MD, XZX-86-006, Aug. 1986.

¹⁵Chobotov, V. A., Spencer, D. B., Schmitt, D. L., Gupta, R. P., Hopkins, R. G., and Knapp, D. T., "Dynamics of Debris Motion and the Collision Hazard to Spacecraft Resulting from an Orbital Breakup," The Aerospace Corp., Los Angeles, CA, SD-TR-88-96, Jan. 1988.

¹⁶"Spacecraft Design Characteristic Manual for the Navy Navigation Satellite System," RCA Corporation, NOOO30-83-C-0155, Feb. 1986.

¹⁷SLAM Test Meetings, Air Force Academy, Dept. of Physics, Colorado Springs, CO, 1989-90; part of ASATJPO test requirements, 1990.

¹⁸Johnson, N. L., "History and Consequences of On-Orbit Break-Ups," *Advances in Space Research*, Vol. 5, No. 2, 1985, pp. 11-19.

¹⁹Su, S.-Y., "On the New Ejecta Velocity vs Size Distribution of Collisional Fragments and Its Effect on Future Space Debris Environment," NASA Internal Memo, July 1986.

²⁰Reynolds, R., "Review of Current Activities To Model and Measure the Orbital Debris Environment in Low-Earth Orbit," Paper III.2.1, Committee on Space Research, XXVII, Helsinki, Finland, July 1988.

²¹Su, S.-Y., "The Velocity Distribution of Collisional Fragments and Its Effect on Future Space Debris Environment," Paper III.2.5, COSPAR XXVII, Helsinki, Finland, July 1988.

²²Chobotov, V., and Spencer, D., private communications, July 1990.

²³Blair, C. E., et al., "Homing Overlay Experiment (HOE) Safety Evaluation Range Safety Study Task 1203," Ford Aerospace and Communications Corporation, Colorado Springs, CO, Aeronautics Division Rept. U-6655, Nov. 1980.

²⁴Nizza, R. S., and Moll, R. L., "HOE Nonnuclear Kill Two-Body Impact Range Safety Debris Evaluation Study," Lockheed Missiles and Space Company, Houston, TX, Rept. LMSC-D767047, Feb. 1981.

²⁵King-Hele, D., *Satellite Orbits in an Atmosphere*, Blackie and Son, London, 1987.

²⁶Badhwar, G. D., and Anz-Meador, P. D., "Determination of the Area and Mass Distribution of Orbital Debris Fragments," *Earth, Moon and Planets* 45, 1989, pp. 29-51.

²⁷Barker, W. N., Eller, T. J., and Herder, L. E., "A New Approach in Treating the Ballistic Coefficient in the Differential Correction Fitting Program," *Astrodynamics Specialist Conference*, Stowe, VT, AAS Paper 89-374, Aug. 7-10, 1989.

²⁸Glover, R. A., Hoots, F. R., and France, R. G., "Ballistic Coeffi-

cient Estimation of Satellite Breakup Debris: Debris Cloud Analyses," *Astrodynamics Specialist Conference*, Stowe VT, AAS Paper 89-377, Aug. 7-10, 1989.

²⁹McKnight, D. S., "Classification of Satellite Breakups by Debris Fragment Lifetimes," *AAS/AIAA Astrodynamics Specialist Conference*, Kalispell, MT, AAS Paper 87-471, Aug. 10-13, 1987.

³⁰Culp, R. D., and McKnight, D. S., "Distinguishing Between Collision-Induced and Explosion-Induced Satellite Breakup Through Debris Analysis," *Astrodynamics* 1985, Vol. 58, Pt. 1, Advances in Astrodynamics Sciences, San Diego, 1986, pp. 739-758.

³¹McKnight, D. S., "The Effect of Breakup Modeling Uncertainties on Space Operations," *AIAA Paper* 91-0097, Jan. 1991.

³²Badhwar, G. D., Tan, A., and Reynolds, R. C., "Velocity Perturbation Distributions in the Breakup of Artificial Satellites," *Journal of Spacecraft and Rockets*, Vol. 27, No. 3, May-June 1990, pp. 299-305.

³³Johnson, N. L., private communications, 1990.

³⁴Johnson, N. L., and Nauer, D. J., "Orbital Debris Detection: Techniques and Issues," *AIAA Paper* 90-1330, April 1990; see also *Journal of Spacecraft and Rockets*, to be published.

³⁵Kling, R., "Postmortem of a Hypervelocity Impact: Summary," Teledyne Brown Engineering, Colorado Springs, CO, CS86-LKD-001, Sept. 1986.

³⁶Johnson, N. L., "The Collision of Satellites 16937 and 16938: A Preliminary Report," Teledyne Brown Engineering, Colorado Springs, CO, CS87-LKD-001, Nov. 1986.

³⁷Mullins, S. A., and Anderson, C. E., "Dissimilar Material Scaling Relationships for Hypervelocity Impact," Defense Nuclear Agency, Alexandria, VA, DNA-TR-89-112, July 1990.

³⁸Ausherman, D. R., Bronstein, M. P., Fink, S. F., and Jaco, C. B., "Starbird Fragmentation Analysis," TRW Rept. 90.k314.5-038, April 1990.

³⁹Brown, C. R., "Collision Debris Model," letter dated Aug. 24, 1990, Applied Physics Laboratory, Laurel, MD, AL-90-d0113, JCH-90-058.

⁴⁰Maclay, T. D., "On the Subject of Mass Distribution Equations," University of Colorado, Boulder, Internal Rept. SD-90-03T, Sept. 1990.

⁴¹Dickey, M. R., and Culp, R. D., "Determining Characteristic Mass for Low-Earth-Orbiting Debris Objects," *Journal of Spacecraft and Rockets*, Vol. 26, No. 6, Nov.-Dec. 1989, pp. 460-464.

⁴²Culp, R. D., and Dickey, M. R., "The Correlation Between Radar Cross Section and Ballistic Coefficient for Orbiting Objects," *AAS/AIAA Astrodynamics Specialist Conference*, Kalispell, MT, AAS Paper 87-474, Aug. 10-13, 1987.

Paul F. Mizera
Associate Editor